Particulate phosphorus hysteresis, loads, and reactivity during the Cyclone Alfred Flood in the Albert River, Southeast Queensland

Maarten Wynants[1,2], Cornelis Verboom[3], Will Bennett[2], Pascal Boeckx[1] and Andrew P. Brooks[2]

1 Isotope Bioscience Laboratory (ISOFYS), Department of Green Chemistry and Technology, Ghent University, 9000 Gent, Belgium. Email: maarten.wynants@ugent.be

2 School of Environment and Science, Griffith University, Gold Coast Campus, 4222, Australia. Email: m.wynants@griffith.edu.au

3 Faculty of Geosciences, Utrecht University, 3584 CB Utrecht, the Netherlands

Key points

- Alfred flood event dominated (~65%) annual particulate phosphorus (PP) export.
- A figure-eight hysteresis pattern reveals multi-phase source activation.
- Initial PP transport is driven by oxide-bound P from bank sediments, while peak discharge disproportionately mobilises more reactive exchangeable P (>50% of event load).
- The exchangeable P pulse is unlikely to originate from cropland fertiliser runoff.

Abstract

Extreme flood events strongly influence soil erosion, water quality, and nutrient export in subtropical river systems, yet their intra-event dynamics and controls on phosphorus sources and reactivity remain poorly understood. We characterised particulate phosphorus (PP) concentration–discharge (PPC–Q) relationships during the March 2025 Tropical Cyclone Alfred flood in the Albert River (southeast Queensland, Australia) using high-frequency rising-stage and grab sampling. PPC exhibited a figure-eight hysteresis pattern (HI = 0.40), indicating sequential activation of distinct phosphorus sources and shifts in hydrological connectivity throughout the hydrograph. An initial first-flush peak at low discharge was dominated by oxide-bound P, consistent with mobilisation of in-channel and bank-derived sediments. A second, larger peak at high discharge coincided with a marked increase in exchangeable P, indicating enhanced mobilisation of highly reactive and bioavailable phosphorus. Event-scale load estimates show that ~199 t of PP were exported, with >50% as exchangeable P. Extrapolation to the annual hydrograph indicates that this single event contributed ~65% of yearly PP export. These results demonstrate that extreme floods not only dominate total PP fluxes but also disproportionately mobilise the most reactive phosphorus fractions. This study highlights the role of non-linear mobilisation processes and hydrological thresholds in controlling phosphorus export. The dominance of short-lived pulses of reactive P during extreme events has important implications for downstream eutrophication risk, particularly under increasing hydroclimatic extremes.

Keywords

Extreme events, hydrochemical connectivity, non-linear mobilisation, reactive phosphorus, eutrophication, Moreton Bay

Introduction

Phosphorus is a key limiting nutrient in freshwater and coastal ecosystems, and its transport in particulate form plays a central role in eutrophication processes worldwide (Haygarth et al., 2005; Jarvie et al., 2013). In subtropical and tropical river systems, particulate phosphorus (PP) often dominates total phosphorus export, particularly during flood events when erosion and sediment mobilisation increase rapidly (Kerr et al., 2011b). Eastern Australian rivers exemplify these dynamics, with extreme floods linked to tropical cyclones and monsoonal systems contributing the majority of annual nutrient export (Cartwright et al., 2025; Olley et al., 2015). Rivers draining to Moreton Bay (southeast Queensland) have experienced increased erosion and sediment yield since European settlement due to land-use change (Coates-Marnane et al., 2016; Kemp et al., 2015; Olley et al., 2015).

Recent large floods have caused widespread bank failures, sediment-laden coastal plumes, and declines in water quality across riverine and coastal environments (Hancock and Caitcheon, 2010; McMahon et al., 2017; Queensland Government, 2025). These pressures are intensified by increasing urbanisation in South East Queensland, increasing reliance on clean water and healthy ecosystems. Moreton Bay and its tributaries support major economic and recreational activities, while surrounding alluvial plains are highly productive agricultural areas. However, the bay is susceptible to phosphorus loading (Eyre and McKee, 2002; Wulff et al., 2011), and increasing phosphorus losses from land to rivers thus pose risks to both water security and agricultural productivity (Council of Mayors, 2015; Healthy Land & Water 2025; Queensland Government, 2025). Quantifying water quality impacts during large floods is therefore critical for effective land and water management (Bieroza et al., 2019; Zou et al., 2023).

PP transport in these systems is largely attributed to sediment mobilisation processes such as riverbank erosion (Fox et al., 2016; Olley et al., 2015). However, wet-dry cycling, sorption of dissolved phosphorus to sediments, and other environmental controls strongly influence PP dynamics along the transport continuum (Kerr et al., 2010; Kerr et al., 2011a), ultimately controlling its ecological impact (Garzon-Garcia et al., 2018). Exchangeable phosphorus fractions are loosely bound, more bioavailable, and can rapidly drive algal blooms once delivered to receiving waters (House, 2003). Despite the importance of extreme events, intra-event variations in PP concentration and reactivity remain poorly understood, largely due to the challenges of high-frequency sampling during floods. Consequently, knowledge of how PP sources and chemical forms evolve over flood hydrographs is limited, particularly in Australian (sub)tropical systems (Blöschl et al., 2019; Drewry et al., 2006). This knowledge caveat on the P transport continuum is increasingly critical given projections of more frequent and more intense storm events under future climates and warmer oceans (Forber et al., 2018).

This study addresses these gaps in understanding of phosphorus dynamics during extreme floods by analysing PP hysteresis behaviour, loads, and geochemical reactivity during the extreme Tropical Cyclone Alfred flood event in the Albert River. We test the hypothesis that extreme flows have a disproportional impact on total PP export but also preferentially mobilise more reactive phosphorus fractions, thereby amplifying downstream ecological risk.

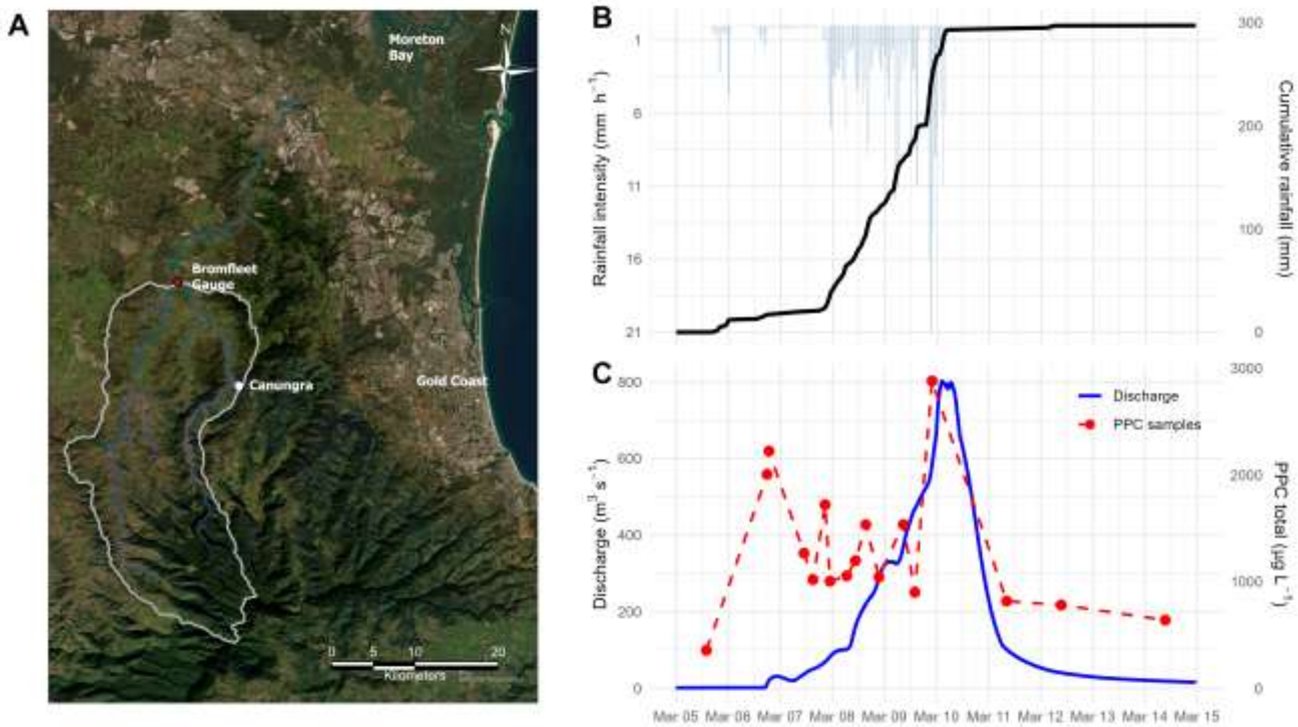

Figure 1 Overview figure the study catchment (A), and detailed storm event rainfall hyetograph (B) and Discharge and total Particulate Phosphorus concentration dynamics and sample times (C)

Material and methods

Study catchment and event

The Albert River in southeast Queensland, Australia, is a flood-prone catchment representative of subtropical river systems in eastern Australia (Figure 1A). The catchment upstream the Bromfleet gauge (145101D; lat: -27.9092, lon: 153.1065) drains 542 km^2, featuring a strong topographic gradient from upland areas through steep intermediate hillslopes to flat alluvial valleys. Annual rainfall ranges from ~790 to 1580 mm, strongly influenced by orography and seasonality, with ~70% falling between October and March. Upland areas are dominated by protected subtropical Gondwana rainforest and wet sclerophyll forest, with thin basalt-derived clay soils. Intermediate hillslopes form a transition zone of mixed lithology and land use, including dry sclerophyll forest, grazing land, and expanding urban areas around Canungra. Soils here range from shallow clays on steep slopes to thicker colluvial duplex soils on foothills. The lower catchment consists of alluvial plains with deep, fertile clay soils and high water availability, supporting intensive agriculture. Extensive land clearing has reduced natural vegetation to narrow remnants. The river is deeply incised into these alluvial deposits, with bank heights exceeding 15 m at Bromfleet.

Tropical Cyclone Alfred (March 2025) produced intense rainfall (Figure 1B) with weekly totals ranging from 180 mm in the lowlands to 700 mm in the uplands, generating a rapid flood response with peak discharge exceeding 800 $m^3 s^{-1}$ (Figure 1C). In the nearly 100-year record of the Bromfleet gauging station, the discharge only crossed the 800 $m^3 s^{-1}$ threshold a total of 21 times (254 hours), highlighting the relative rarity of the studied event.

Sampling strategy

At the Bromfleet river discharge gauging station, suspended sediment was collected using a series of rising stage samplers (RSS) installed at 1.4m, 2.3m, 3.6m, 4.5m, 5.7m, 6.5m, 7.5m, 9.1m, 11.1m, 12.1m, 13.1m, and 14.1m above the channel bed, supplemented with grab samples during baseflow conditions before and after the event, and falling-stage conditions at 7.6m, 3.9m and 2.1m above the channel bed. This approach enabled reconstruction of PP concentration dynamics across the full discharge range (Table 1).

Table 1 Storm event samples with datetimes, associated hydrograph, and SSC and PPC fractions

Sample Type	Sampling datetime	Discharge (m3 s^{-1})	SSC (mgL^{-1})	PP_ex (µg L^{-1})	PP_car (µg L^{-1})	PP_oxtot (µg L^{-1})	PP_rec (µg L^{-1})	PP_tot (µg L^{-1})
Base 1	05/03/2025 14:00	1.6	372.5	3.0	296.9	86.3	16.0	402.2
Base 2	05/03/2025 14:04	1.6	323.5	2.6	257.9	74.9	13.9	349.2
Base 3	05/03/2025 14:08	1.6	339.6	1.1	231.8	73.3	13.1	319.3
RSS1.4	06/03/2025 17:55	10.8	1286.8	51.9	353.3	1492.9	107.9	2005.9
RSS2.3	06/03/2025 18:50	21.0	1415.9	99.8	325.4	1664.2	135.3	2224.7
RSS3.6	07/03/2025 10:55	36.8	800	133.4	243.5	776.6	112.8	1266.3
RSS4.5	07/03/2025 15:05	50.1	645.2	152.4	179.5	589.1	98.0	1019.0
RSS5.7	07/03/2025 20:40	69.3	495.4	653.4	624.5	353.5	90.4	1721.8
RSS6.5	07/03/2025 22:55	82.9	733.3	129.0	168.7	608.6	98.2	1004.5
RSS7.5	08/03/2025 06:35	101.9	616.7	228.8	197.4	512.7	115.7	1054.6
RSS9.1	08/03/2025 10:40	161.2	533.3	208.9	264.7	588.3	135.7	1197.6
RSS10.1	08/03/2025 15:25	220.2	683.3	267.6	339.1	753.7	173.9	1534.4
RSS11.1	08/03/2025 21:25	286.4	448.3	450.5	211.2	293.7	87.7	1043.2
RSS12.1	09/03/2025 08:40	370.7	500	272.4	521.8	602.6	138.9	1535.8
RSS13.1	09/03/2025 14:00	468.6	467.7	232.0	184.2	406.2	78.1	900.6
RSS14.1	09/03/2025 21:55	584.4	1294.1	2029.9	274.2	396.1	181.2	2881.5
FS7.5	11/03/2025 08:15	101.9	392	200.3	214.7	343.5	59.4	817.8
FS3.8	12/03/2025 09:25	40.4	470.8	62.6	173.1	493.1	52.6	781.5
FS2.1A	14/03/2025 09:32	18.6	480.8	39.0	171.5	479.9	47.7	738.0
FS2.1B	14/03/2025 09:35	18.6	363.6	20.1	141.6	344.7	35.1	541.5

Laboratory analysis

The volume of the RSS samples was recorded using a measuring cylinder, and the samples were subsequently oven-dried at 60°C to infer the total mass of the suspended sediment. Suspended Sediment Concentration (SSC) was calculated by dividing mass of sediment by volume of sampled water. Dried suspended sediment samples were disaggregated and sieved to <63 µm for further analysis.

Sediment-associated phosphorus fractions were extracted following a modified protocol based on Poulton and Canfield (2005), which while originally developed for iron mineralogy, is suitable for functional elemental fractions in (sub)tropical soils with high oxide content. It sequentially extracts the sediment, dividing sediment-associated P in 6 operational groups: (1) exchangeable fraction (ex; 1 M

$MgCl_2$ buffered at pH 7 for 2 hours at room temperature), (2), carbonates (car; 1 M $CH_3COONa.3H_2O$ buffered at pH 4.5 for 24 hours at room temperature), (3) easily reducible oxides (ox1; 1 M $NH_2OH{\cdot}HCl$ in 25% CH_3COOH for 48 hours at room temperature), (4) crystalline oxides (ox2; 50 g L^{-1} $Na_2S_2O_4$ solution buffered at pH 4.8 for 2 hours at room temperature), (5) poorly reducible oxides (ox3; 0.2 M $(NH_4)_2C_2O_4.H_2O$ + 0.17 M $C_2H_2O_4.2H_2O$ buffered at pH 3.2 for 6-12 hours in the dark at room temperature), (6) the recalcitrant fraction (rec; reverse aqua regia with 3:1 HNO_3 and HCl for 24 hours at roughly 95°C). All extracts were analysed by Inductively Coupled Plasma Mass Spectrometry (ICP-MS; Agilent 8900, Agilent Technologies, Santa Clara, CA, USA), yielding concentrations (µg/l), which were then recalculated to dry weight P concentration in mg kg^{-1} of sediment using the original noted weight, the reagent volume, and the dilution factor. Finally, the particulate phosphorus concentrations (PPC) per sample were obtained by multiplying the obtained SSC values with the dry weight concentrations of each phosphorus fraction, yielding PPC of the fractions and total in mg l^{-1}. It can be assumed that the dissolved P got bound to particles during the drying and was subsequently extracted as exchangeable PP.

Data analysis of PP Hysteresis and fractional loads

A concentration-discharge loop was plotted and visually interpreted for shape and direction. Clockwise hysteresis indicates higher concentrations on the rising limb than on the falling limb at equivalent discharges, suggesting rapid mobilisation of proximal or readily available sources. Counter-clockwise hysteresis indicates higher concentrations on the falling limb, suggesting delayed delivery from more distal sources or in-stream processing. More complex figure-eight loops may indicate multiple source activations, shifts in hydrological connectivity, or changes in dominant transport pathways during storm events (Jing et al., 2025; Lloyd et al., 2016b). The event-scale Hysteresis Index (HI) was calculated following equation 1 of Lloyd et al. (2016a), using normalised discharge and concentration data of SSC and PPC to quantify differences between the rising and falling limbs of the hydrograph:

$$HI = \frac{1}{n}\sum_{i=1}^{n}\frac{C_{r,\,i} + C_{f,\,i}}{C_{r,\,i} - C_{f,\,i}} \tag{1}$$

where $C_{r,\,i}$ and $C_{f,i}$ are the mean normalised concentrations separated for the rising and falling limbs, within discharge bin i, and n is the total number of discharge bins.

To characterise short-term shifts in hysteretic dynamics throughout the storm, the raw stepwise hysteresis slope (HS) was also calculated for each successive sample as per equation 2:

$$HS_{step,\,i} = \frac{\Delta C_i}{\Delta Q_i} \tag{2}$$

Positive HS values indicate PPC and Q values rise together, while negative values indicates opposite behaviours. The higher the values, the stronger the concentration or dilution response.

Spearman correlation tests were performed on the PPC fractions and relative proportions with Q, rainfall intensity, and the HS as predictor.

Instantaneous particulate phosphorus (PP) loads were calculated by multiplying PP concentration (PPC) by discharge at each sampling point. Time-integrated loads were then derived by interpolating between consecutive timesteps. The PPC-Q hysteresis observed during the Alfred storm event was extrapolated to the full 2024-2025 hydrological year. Five hysteresis states were defined based on hydrograph stage and limb position: (i) baseflow (<1 m stage), (ii) rising 1 (1-3 m on the rising limb), (iii) rising 2 (3-13.5 m on the rising limb), (iv) peak (13.5-17 m on either limb), and (v) falling (13.5-1 m on the falling limb). Mean measured PP concentrations for each state were used to assign PPC values across the entire hydrological record, enabling estimation of annual PP loads and evaluation of the relative contribution of the Alfred event. All load analyses were conducted for total PP and disaggregated by functional reactivity groups, allowing assessment of their relative contributions across both the event and the annual scale.

Results and discussion

Event-scale hysteresis, phosphorus loads, and source activation

The event-scale hysteresis index (HI = 0.40) indicates predominantly clockwise behaviour for PP. PPC exhibited two distinct peaks, forming a figure-eight hysteresis loop (Figure 2), which reflects complex intra-event dynamics with multiple phases of PP mobilisation rather than a simple first-flush response. The initial peak occurred early in the event and showed the steepest hysteresis slopes, consistent with a strong first-flush effect. This phase was primarily driven by elevated suspended sediment concentrations (SSC), indicating rapid mobilisation of in-channel alluvial sediments and associated PP, likely originating from previously collapsed riverbank material. The dominance of oxide-bound PP during this phase supports this interpretation. A second, larger PPC peak coincided with peak discharge and was driven by both high SSC and elevated sediment-P concentrations. Its greater magnitude suggests the activation of additional or more hydrologically connected P sources during peak flow conditions.

Phosphorus fractionation remained relatively stable throughout most of the hydrograph but shifted markedly at peak discharge, with a pronounced increase in exchangeable P (PP_ex) (Figure 3). During baseflow, PP was dominated by carbonate-associated P (PP_car), whereas smaller flood events were characterised by oxide-associated P (PP_ox). Although no significant relationship was observed between discharge (Q) and total PP concentration (PP_total), strong positive correlations were found between Q and PP_ex and its proportional contribution (p-value ~ 0). Rainfall intensity was positively correlated with PP_total ($p = 0.02$), with particularly strong relationships for PP_ex (p-value ~ 0) and PP_rec ($p = 0.005$). In contrast, the proportion of PP_ox showed a significant negative relationship with Q ($p = 0.02$), whereas the overall hysteresis slope was positively correlated only with PP_total and PP_car. Together, these patterns indicate clear differences in PP sources between peak events: the initial peak was dominated by PP_ox, while the second was dominated by PP_ex. This suggests that peak flows not only transported greater PP loads but also higher proportions of bioavailable fractions. The dominance of PP_ex during peak rainfall and discharge may reflect (i) preferential mobilisation of labile P through rainfall-driven erosion, (ii) increased hydrological connectivity to more distal sediment sources enriched in labile P, or (iii) most plausibly, inputs from untreated sewage overflows or fertiliser runoff during intense rainfall (Kerr et al., 2011b).

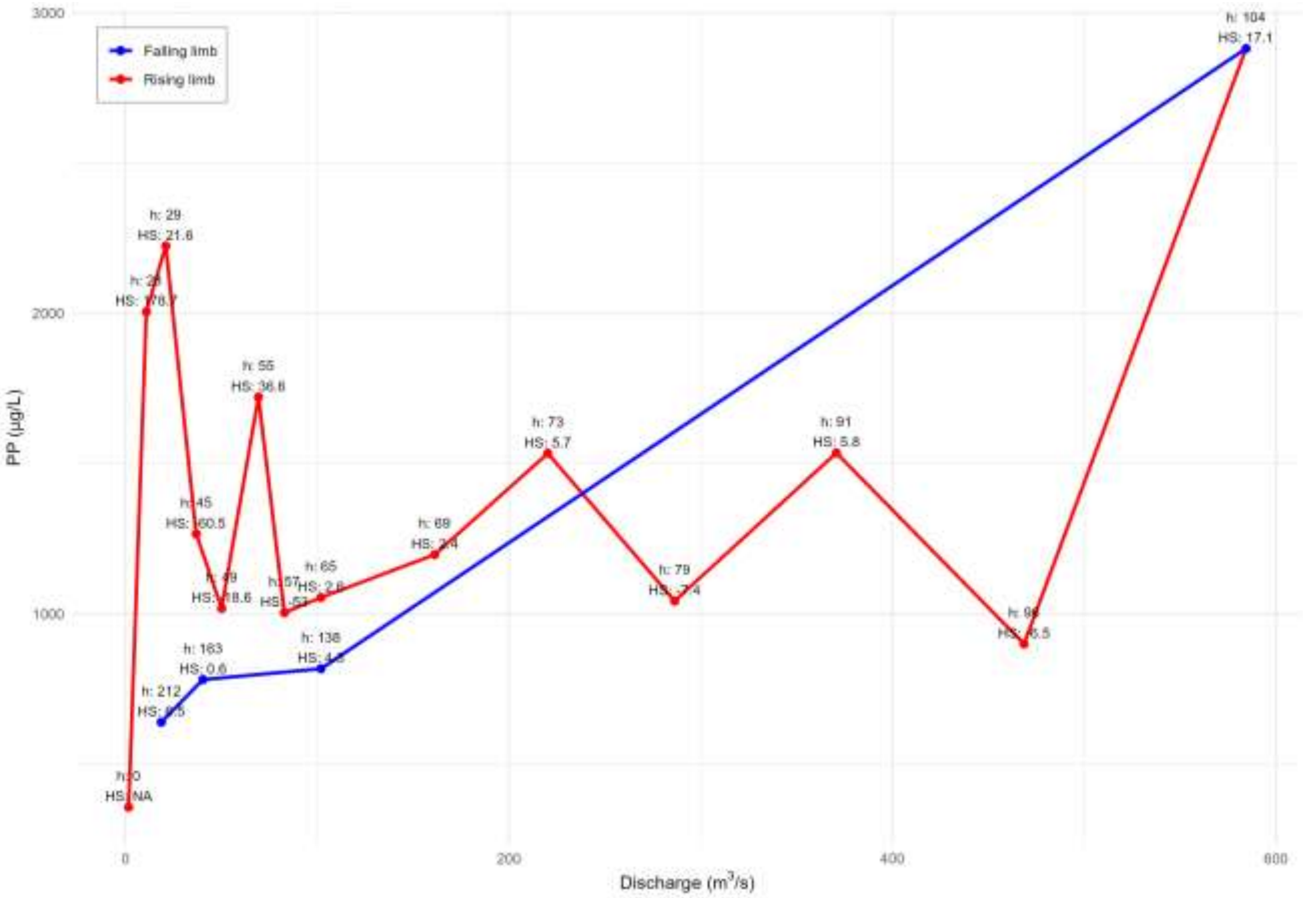

Figure 2 PPC-Q hysteresis loop with the rising limb in red and the falling limb in blue. Each dot represent a sampling timepoint with indication of the hour (h) and hysteresis slope (HS)

PP loads increased nonlinearly with discharge, with the majority of export occurring within a short window around peak flow (Figure 3). Total PP export during the Alfred flood at Bromfleet was approximately 199 t, with ~53% exchangeable P (~106 t), ~25% oxide-bound P (~49 t), ~15% carbonate-bound P (~30 t), and ~7% recalcitrant P (~14 t). This distribution indicates that most exported PP was highly reactive and therefore likely bioavailable. Extrapolation of the observed hysteresis relationships to the July 2024-June 2025 hydrograph suggests that the Alfred flood contributed approximately 65% of the annual PP export, highlighting the dominant role of extreme events in system-scale P budgets. Despite contributing primarily during high-flow conditions, exchangeable P was the largest annual fraction (38.6%), followed by oxide-bound P (33.9%), which dominated smaller floods, and carbonate-bound P (20.6%), which was most important during baseflow. Overall, these findings highlight the critical role of non-linear phosphorus source activation, mobilisation, and hydrological connectivity thresholds during extreme events (Kerr et al., 2011b).

Methodological uncertainties

Due to the exponential stage-discharge relationship and the lack of sampling at the highest river stage during Cyclone Alfred, the true PPC peak was likely not captured. In addition, safety constraints prevented sampling during the initial falling stage, creating gaps in the PPC–discharge hysteresis pattern. Placement of the RSS on vegetated banks may have further contributed to underestimation, as increased surface roughness can reduce local transport capacity and produce lower concentrations than in the channel centre (Errico et al., 2018). The rapid deployment of the field setup in response to the cyclone's unpredictable trajectory also constrained sampling design. Future similar studies would benefit from employing automated samplers to provide continuous, high-frequency sampling throughout the hydrograph from a consistent channel location. Permanent autosampler installations would also improve temporal coverage across smaller events and dry-season baseflow conditions

(Doriean et al., 2020). Additional uncertainty arises from assumptions used in load calculations. Event peak classification was based on the observed peak sediment load during Cyclone Alfred, despite the true discharge peak not being sampled. As a result, peak PPC values and total PP loads were likely underestimated (Malutta et al., 2020). For other events, PPC values during Rising Stage 1 and Rising Stage 2 were assumed to match those measured during Alfred, while baseflow concentrations were derived from wet-season observations and likely overestimate dry-season conditions. Collectively, these factors suggest that the contribution of the Cyclone Alfred event to annual sediment and phosphorus (P) loads is an underestimation (Carpenter et al., 2018; Valkama and Ruth, 2017).

Implications for catchment soil and water management

The peak discharge during the extreme Cyclone Alfred flood represents a critical “hot moment” for both total PP losses and reactivity. Our results show that oxide-bound P, likely derived from mobilised riverbank material, dominates during the early rising and late falling stages of the hydrograph. Although managing bank erosion remains important for long-term local water quality (Olley et al., 2015), these oxide fractions are relatively less reactive and therefore less likely to drive rapid downstream impacts.

In contrast, most PP transport occurs during the short peak discharge window, which is dominated by the highly bioavailable PP_ex. This fraction accounts for over 50% of total event loads, and annual extrapolations further emphasise the disproportionate importance of such extreme events. Consequently, the majority of PP exported to Moreton Bay occurs as short pulses of highly reactive P, posing a substantial risk for downstream algal blooms. Based on phosphate fertiliser prices of approximately 4.3–5.5 AUD per kg P (ABARES, 2025), the estimated loss of 199 t of P corresponds to an economic value of roughly $0.85–1.1 million AUD. However, parallel results from sediment tracing indicates a shift in source contributions during peak flow toward intermediate hillslope soils that are often characterised by dispersive subsoils, rather than fertilised alluvial cropland. Likewise, none of the analysed soils had similar high proportion of PP_ex. This reduces the likelihood that the PP_ex pulse originates from diffuse cropland runoff. Instead, point source contributions might be more likely, such as livestock pen effluent and slurry storage runoff. Rapid urban expansion in Canungra, associated with increased land clearing, soil disturbance, and pressure on stormwater and sewage systems, can also suggests that part of the reactive PP pulse reflects inputs from urban sewage overflows and/or mobilisation of recently exposed dispersive soils with preferential mobilisation of the PP_ex fraction during intense rainfall.

Overall, these findings demonstrate that management strategies based on typical flow conditions or smaller events are insufficient to mitigate downstream phosphorus loading (Bieroza et al., 2019; Zou et al., 2023). Effective approaches must instead target highly reactive P pools and enhance the resilience of land and water management systems to stochastic extreme rainfall events (Forber et al., 2018). Low-hanging fruits management interventions include improving sewage infrastructure capacity and reducing runoff and erosion from exposed soils in both urban and agricultural settings.

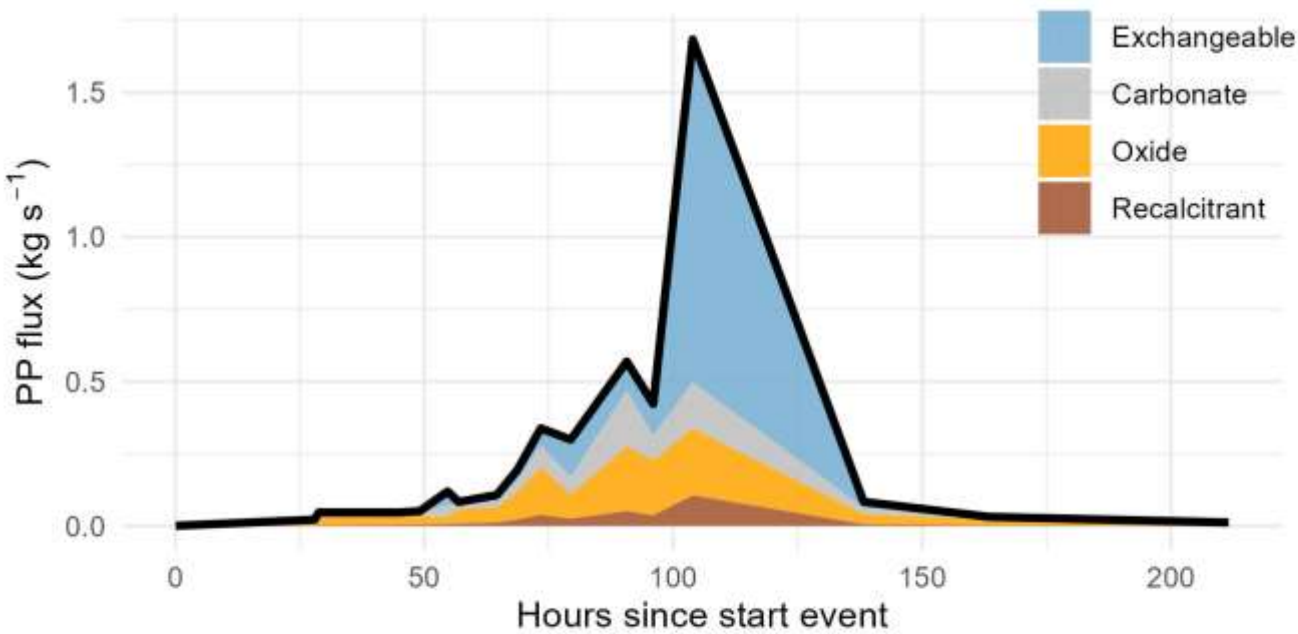

Figure 3 Instantaneous PP fractional load changes over the course of the Alfred storm event

Conclusions

Extreme flood events in subtropical rivers act as critical "hot moments" that disproportionately control both the magnitude and reactivity of particulate phosphorus (PP) export. The Cyclone Alfred event contributed ~65% of annual PP export (~199 t), with over half of this load consisting of highly bioavailable exchangeable P (PP_ex). This demonstrates that extreme flows not only mobilise large quantities of PP but also preferentially transport its most reactive fractions. The observed figure-eight PPC–Q hysteresis (HI = 0.40) reveals multi-phase mobilisation dynamics rather than a simple first-flush response. Early in the event, transport was dominated by oxide-bound P (PP_ox), consistent with mobilisation of alluvial bank sediments. In contrast, peak discharge triggered a marked shift toward PP_ex dominance, indicating activation of more reactive phosphorus sources. These results highlight the importance of non-linear thresholds in P source activation during extreme events. This reactive PP pulse most likely originates from potential urban or livestock sewage overflows, and recently disturbed dispersive subsoils. This requires a shift in focus of catchment management beyond cropland and river bank restoration, to include rapidly urbanising areas and stressed infrastructure. Overall, these findings show that strategies based on typical flow conditions underestimate both PP export and eutrophication risk. Effective management must target reactive P pools, reduce erosion from exposed soils, and improve stormwater and sewage system resilience in urban and livestock facilities, particularly under increasingly frequent extreme rainfall events.

Acknowledgements

This work was supported by the Marie Skłodowska-Curie Actions (MSCA) under grant agreement No. 101109315 (AsFoRESEEN). The authors acknowledge the contribution of Ryan Stewart from the Environmental Research Facility at Griffith University for his support of the ICP-MS analysis.

References

ABARES, 2025. Agricultural Commodities Report: June Quarter 2025, Department of Agriculture, Fisheries and Forestry, Canberra, Australia.

Bieroza, M., Bergström, L., Ulén, B., Djodjic, F., Tonderski, K., Heeb, A., Svensson, J., Malgeryd, J., 2019. Hydrologic extremes and legacy sources can override efforts to mitigate nutrient and sediment losses at the catchment scale. *Journal of environmental quality*, 48(5), 1314-1324.

Blöschl, G., Bierkens, M.F., Chambel, A., Cudennec, C., Destouni, G., Fiori, A., Kirchner, J.W.,

McDonnell, J.J., Savenije, H.H., Sivapalan, M., 2019. Twenty-three unsolved problems in hydrology (UPH)–a community perspective. *Hydrological Sciences Journal*, 64(10), 1141-1158.
Carpenter, S.R., Booth, E.G., Kucharik, C.J., 2018. Extreme precipitation and phosphorus loads from two agricultural watersheds. *Limnology and Oceanography*, 63(3), 1221-1233.
Cartwright, P., Genson, A., Waltham, N., 2025. The effect of wet season river flows on flood plume distribution across northern Australia; contribution to coastal productivity, and future extent under climate change. *Regional Studies in Marine Science*, 89, 104307.
Coates-Marnane, J., Olley, J., Burton, J., Sharma, A., 2016. Catchment clearing accelerates the infilling of a shallow subtropical bay in east coast Australia. *Estuarine, Coastal and Shelf Science*, 174, 27-40.
Council of Mayors, 2015. South East Queensland Resilient Rivers Initiative Regional Strategy 2015–2025, Council of Mayors (South East Queensland), Brisbane, Australia.
Doriean, N.J., Brooks, A.P., Teasdale, P.R., Welsh, D.T., Bennett, W.W., 2020. Suspended sediment monitoring in alluvial gullies: A laboratory and field evaluation of available measurement techniques. *Hydrological Processes*, 34(16), 3426-3438.
Drewry, J., Newham, L., Greene, R., Jakeman, A., Croke, B., 2006. A review of nitrogen and phosphorus export to waterways: context for catchment modelling. *Marine and Freshwater Research*, 57(8), 757-774.
Errico, A., Pasquino, V., Maxwald, M., Chirico, G., Solari, L., Preti, F., 2018. The effect of flexible vegetation on flow in drainage channels: Estimation of roughness coefficients at the real scale. *Ecological Engineering*, 120, 411-421.
Eyre, B.D., McKee, L.J., 2002. Carbon, nitrogen, and phosphorus budgets for a shallow subtropical coastal embayment (Moreton Bay, Australia). *Limnology and Oceanography*, 47(4), 1043-1055.
Forber, K., Withers, P., Ockenden, M., Haygarth, P., 2018. The phosphorus transfer continuum: A framework for exploring effects of climate change. *Agricultural & Environmental Letters*, 3(1), 180036.
Fox, G.A., Purvis, R.A., Penn, C.J., 2016. Streambanks: A net source of sediment and phosphorus to streams and rivers. *Journal of Environmental Management*, 181, 602-614.
Garzon-Garcia, A., Burton, J., Franklin, H.M., Moody, P.W., De Hayr, R.W., Burford, M.A., 2018. Indicators of phytoplankton response to particulate nutrient bioavailability in fresh and marine waters of the Great Barrier Reef. *Science of the Total Environment*, 636, 1416-1427.
Hancock, G., Caitcheon, G., 2010. Sediment sources and transport to the Logan–Albert River estuary during the January 2008 flood event, CSIRO Water for a Healthy Country National Research Flagship, Australia.
Haygarth, P.M., Condron, L.M., Heathwaite, A., Turner, B.L., Harris, G., 2005. The phosphorus transfer continuum: linking source to impact with an interdisciplinary and multi-scaled approach. *Science of the Total Environment*, 344(1-3), 5-14.
Healthy Land & Water 2025. Report Card Catchment Summaries 2025, Healthy Land & Water.
House, W.A., 2003. Geochemical cycling of phosphorus in rivers. *Applied Geochemistry*, 18(5), 739-748.
Jarvie, H.P., Sharpley, A.N., Withers, P.J., Scott, J.T., Haggard, B.E., Neal, C., 2013. Phosphorus mitigation to control river eutrophication: murky waters, inconvenient truths, and “postnormal” science. *Journal of environmental quality*, 42(2), 295-304.
Jing, T., Zeng, Y., Fang, N., Dai, W., Shi, Z., 2025. A review of suspended sediment hysteresis. *Water Resources Research*, 61(1), e2024WR037216.
Kemp, J., Olley, J.M., Ellison, T., McMahon, J., 2015. River response to European settlement in the subtropical Brisbane River, Australia. *Anthropocene*, 11, 48-60.
Kerr, J.G., Burford, M., Olley, J., Udy, J., 2010. The effects of drying on phosphorus sorption and speciation in subtropical river sediments. *Marine and Freshwater Research*, 61(8), 928-935.
Kerr, J.G., Burford, M., Olley, J., Udy, J., 2011a. Phosphorus sorption in soils and sediments: implications for phosphate supply to a subtropical river in southeast Queensland, Australia. *Biogeochemistry*, 102(1), 73-85.
Kerr, J.G., Burford, M.A., Olley, J.M., Bunn, S.E., Udy, J., 2011b. Examining the link between terrestrial

and aquatic phosphorus speciation in a subtropical catchment: the role of selective erosion and transport of fine sediments during storm events. *Water Research*, 45(11), 3331-3340.

Lloyd, C.E., Freer, J.E., Johnes, P.J., Collins, A., 2016a. Testing an improved index for analysing storm discharge–concentration hysteresis. *Hydrology and Earth System Sciences*, 20(2), 625-632.

Lloyd, C.E., Freer, J.E., Johnes, P.J., Collins, A., 2016b. Using hysteresis analysis of high-resolution water quality monitoring data, including uncertainty, to infer controls on nutrient and sediment transfer in catchments. *Science of the Total Environment*, 543, 388-404.

Malutta, S., Kobiyama, M., Chaffe, P.L.B., Bonumá, N.B., 2020. Hysteresis analysis to quantify and qualify the sediment dynamics: State of the art. *Water Science and Technology*, 81(12), 2471-2487.

McMahon, J.M., Olley, J.M., Brooks, A.P., Smart, J.C., Rose, C.W., Curwen, G., Spencer, J., Stewart-Koster, B., 2017. An investigation of controlling variables of riverbank erosion in sub-tropical Australia. *Environmental Modelling & Software*, 97, 1-15.

Olley, J., Burton, J., Hermoso, V., Smolders, K., McMahon, J., Thomson, B., Watkinson, A., 2015. Remnant riparian vegetation, sediment and nutrient loads, and river rehabilitation in subtropical Australia. *Hydrological Processes*, 29(10), 2290-2300.

Poulton, S.W., Canfield, D.E., 2005. Development of a sequential extraction procedure for iron: implications for iron partitioning in continentally derived particulates. *Chemical Geology*, 214(3-4), 209-221.

Queensland Government, 2025. Queensland State of the Environment Report 2024, Department of the Environment, Tourism, Science and Innovation.

Valkama, P., Ruth, O., 2017. Impact of calculation method, sampling frequency and hysteresis on suspended solids and total phosphorus load estimations in cold climate. *Hydrology Research*, 48(6), 1594-1610.

Wulff, F., Eyre, B.D., Johnstone, R., 2011. Nitrogen versus phosphorus limitation in a subtropical coastal embayment (Moreton Bay; Australia): Implications for management. *Ecological Modelling*, 222(1), 120-130.

Zou, X.-Y., Peng, X.-Y., Zhao, X.-X., Chang, C.-P., 2023. The impact of extreme weather events on water quality: International evidence. *Natural Hazards*, 115(1), 1-21.